

Supporting information

Single Component Lanthanide Hybrids Based on Metal–Organic Framework Phosphor for Near-Ultraviolet White Light LED

Yan-Wu Zhao[†], Fu-Qiang Zhang[†], and Xian-Ming Zhang^{†‡*}

†School of Chemistry & Material Science, Shanxi Normal University Linfen 041004, P. R. China.

‡Institute of crystalline materials, Shanxi University, Taiyuan 030006, P. R. China

Correspondence to: zhangxm@dns.sxnu.edu.cn.

Contents

Section S1 Energy levels of Calculation with free ligand.....	S-2
Section S2 ICP analysis of doping LnMOF.....	S-4
Section S3 Single crystal data and structure plots.....	S-5
Section S4 PXRD patterns and IR spectra of partial MOF.....	S-8
Section S5 EDS spectrum of the doping LnMOF.....	S-9
Section S6 TGA of Gd(CPOMBA)(H ₂ O) ₂ ·nH ₂ O.....	S-10
Section S7 Excitation and Emission spectra of free ligand, single and doping LnMOF.....	S-11
Section S8 CIE coordinates of doping LnMOF.....	S-14
Section S9 Photoluminescent decay curve of doping LnMOF.....	S-16
Section S10 quantum yield of doping LnMOF.....	S-18
Section S11 Photographs of LEDs and optical photographs of crystal.....	S-19
Section S12 Fabrication of UV WLED.....	S-20
References.....	S-21

Section S1. Energy levels of Calculation with free ligand

Energy levels of Calculation

1. Triplet excited state calculation: the molecular geometry of free ligand H₃CPOMBA was optimized by using Gaussian09 software at the B3LYP/6-31G* level, as shown in Figure S12. The energy of the lowest triplet excited state of H₃CPOMBA was calculated to be 2.873595 eV (${}^3\pi\pi^* = 23177 \text{ cm}^{-1}$) using the time-dependent DFT approach¹.

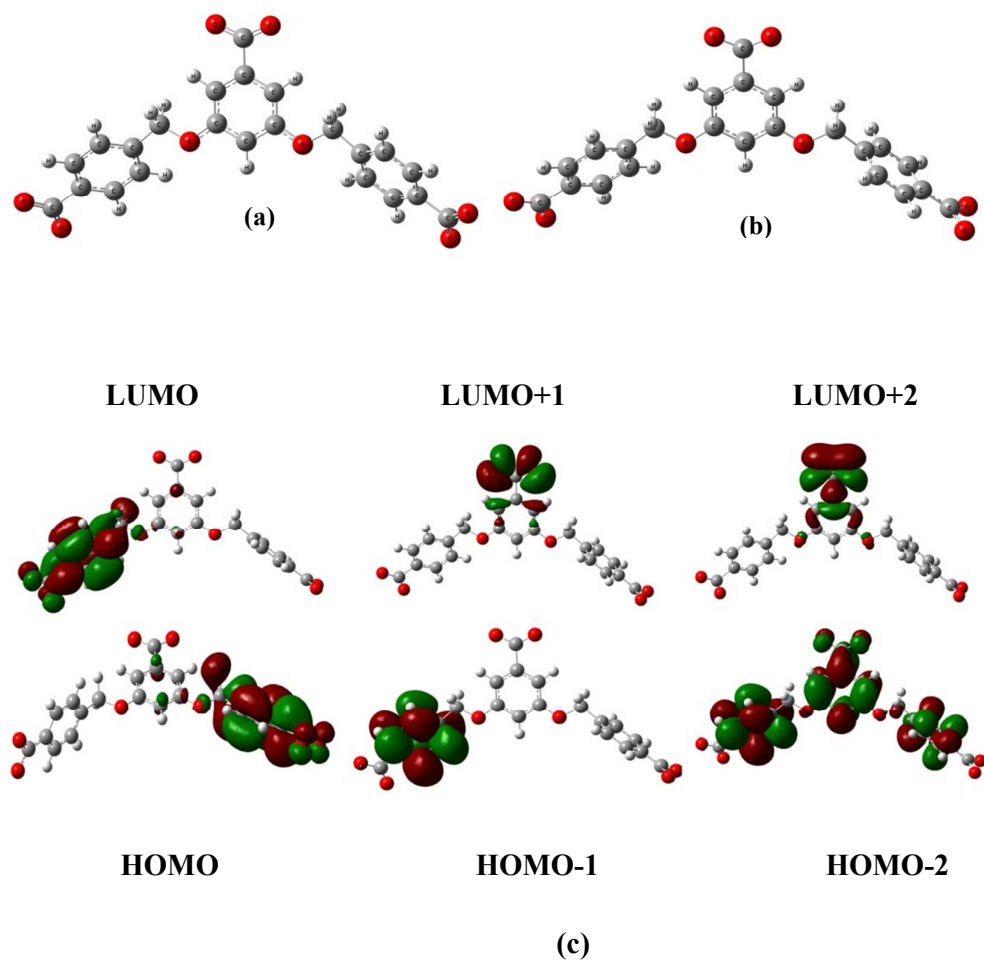


Figure S1. (a) Optimized molecular geometry of free ligand H₃CPOMBA at the ground state; (b) optimized molecular geometry of free ligand H₃CPOMBA at the lowest triplet excited state; (c) Contour plots of the frontier orbitals of free ligand H₃CPOMBA at the lowest triplet excited state.

2. The singlet ($^1\pi\pi^*$) energy levels of H₃CPOMBA (331nm, $^1\pi\pi^* = 30215 \text{ cm}^{-1}$) is estimated by referring to its wavelengths of UV-vis absorbance edges

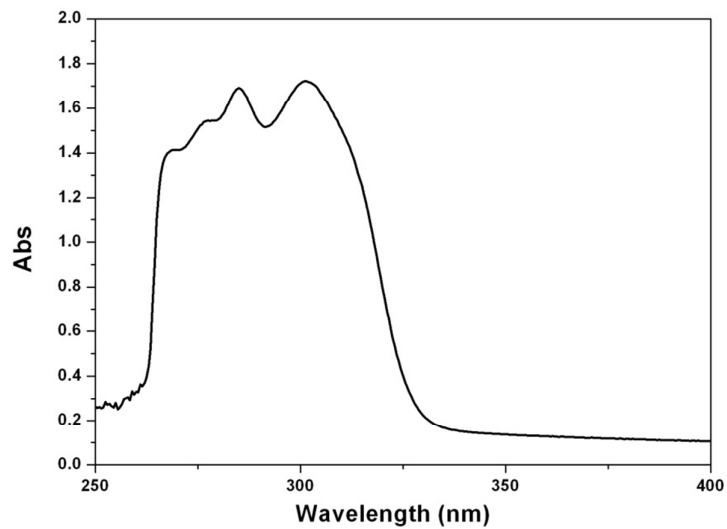


Figure S2. UV absorption spectra of the H₃CPOMBA in DMF solution.

Section S2. ICP analysis of doping LnMOF

Instrumentation: The analytical measurements were made with an ICP OES, model Optima 8000 DV (Perkin-Elmer), equipped with a solid-state segmented double-CCD detectors, an Echelle grating, a peristaltic pump, a crossflow nebulizer coupled to a Scott spray chamber, and a plasma torch. The operational parameters used for the analytical measurements were radio frequency power of 1300 W, nebulization flow rate of 0.8 L/min, auxiliary argon flow rate of 0.5 L/min, plasma argon flow rate of 15.0 L/min, sample flow rate of 1.0 L/min, and read delay of 30 s.

Table S1. The molar ratio of the Tb/Eu in $\text{Eu}_{0.045}\text{Tb}_{0.955}\text{CPOMBA}$ and La/Eu/Tb in $\text{La}_{0.6}\text{Eu}_{0.1}\text{Tb}_{0.3}\text{CPOMBA}$ product by ICP analysis.

sample	The molar ratio of the starting Tb/Eu (or La/Eu/Tb) salt	The ratio by ICP analysis
$\text{Eu}_{0.045}\text{Tb}_{0.955}\text{CPOMBA}$	Eu/Tb 0.045:0.955	0.044:0.956
$\text{La}_{0.6}\text{Eu}_{0.1}\text{Tb}_{0.3}\text{CPOMBA}$	La/Eu/Tb 0.6:0.1:0.3	0.612:0.10:0.298

Section S3. Single crystal data and Structural plots

Table S2. Cell parameters of LnCPOMBA (Ln = La³⁺, Ce³⁺, Pr³⁺, Nd³⁺, Sm³⁺, Eu³⁺, Gd³⁺, Tb³⁺, Ho³⁺, Er³⁺, and Tm³⁺) and co-doped complexes Eu_{0.045}Tb_{0.955}CPOMBA (**1**) and La_{0.6}Eu_{0.1}Tb_{0.3}CPOMBA (**2**).

Compound	<i>a</i> (Å)	<i>b</i> (Å)	<i>c</i> (Å)	α	β	γ	<i>V</i> (Å ³)
LaCPOMBA	13.69(8)	24.01(11)	8.43(5)	90	104.75(2)	90	2698(2)
CeCPOMBA	13.74(6)	23.97(7)	8.48(3)	90	104.591(6)	90	2711(3)
PrCPOMBA	13.71(5)	24.11(10)	8.51(2)	90	104.12(9)	90	2702(3)
NdCPOMBA	13.59(3)	23.59(9)	8.54(3)	90	104.38(6)	90	2689(2)
SmCPOMBA	13.61(5)	24.05(4)	8.59(6)	90	104.71(10)	90	2718(2)
EuCPOMBA	13.78(9)	24.104(14)	8.44(5)	90	104.833(11)	90	2709(3)
GdCPOMBA	13.86(19)	24.088(3)	8.43(12)	90	104.557(2)	90	2723.5(7)
TbCPOMBA	13.80(11)	24.032(19)	8.45(7)	90	104.521(2)	90	2712.6(4)
HoCPOMBA	13.72(2)	23.99(2)	8.47(13)	90	104.73(14)	90	2697(2)
ErCPOMBA	13.74(14)	23.98(2)	8.44(9)	90	104.52(9)	90	2692(1)
TmCPOMBA	13.79(10)	23.90(18)	8.41(7)	90	104.255(10)	90	2687.8(4)
Complex 1	13.77(10)	24.12(6)	8.51(6)	90	104.634(5)	90	2710(3)
Complex 2	13.68(9)	23.98(8)	8.49(8)	90	104.558(6)	90	2705(3)

Table S3. Crystal data and structural refinement for compound LnCPOMBA (Ln= Eu³⁺, Gd³⁺, Tb³⁺ and Tm³⁺).

compound	EuCPOMBA	TbCPOMBA	TmCPOMBA	GdCPOMBA
Formula	C ₂₃ H ₁₉ EuO ₁₀	C ₂₃ H ₁₉ TbO ₁₀	C ₂₃ H ₁₉ TmO ₁₀	C ₂₃ H ₁₉ GdO ₁₀
Formula weight	607.34	614.30	624.31	612.63
T (K)	293(2)	293(2)	293(2)	298(2)
Crystal system	monoclinic	monoclinic	monoclinic	monoclinic
Space group	C2/m	C2/m	C2/m	C2/m
Wavelength (Å)	0.71073	0.71073	0.71073	0.71073
<i>a</i> (Å)	13.78(9)	13.8044(11)	13.7892(10)	13.8599(19)
<i>b</i> (Å)	24.104(14)	24.0322(19)	23.8999(18)	24.088(3)
<i>c</i> (Å)	8.437(5)	8.4465(7)	8.4148(7)	8.4281(12)
α (°)	90	90	90	90
β (°)	104.833(11)	104.521(2)	104.2550(10)	104.557(2)
γ (°)	90	90	90	90
V(Å ³)	2709(3)	2712.6(4)	2687.8(4)	2723.5(6)
Z	4	4	4	4
<i>D</i> _{calc} (g cm ⁻³)	1.489	1.504	1.543	1.484
μ (mm ⁻¹)	2.363	2.654	3.349	2.482
<i>F</i> (000)	1200.0	1208.0	1224.0	1188.0
GOF on F ²	1.040	1.137	1.116	1.166
Final R	R ₁ ^a = 0.0780	R ₁ ^a = 0.0578	R ₁ ^a = 0.0559	R ₁ ^a = 0.0531
wR ₂ ^b [<i>I</i> >2 σ (<i>I</i>)]	0.2131	0.1682	0.1648	0.1603

$${}^a R_1 = \sum ||F_0| - |F_c|| / \sum |F_0|; {}^b wR_2 = [\sum w(F_0^2 - F_c^2)^2 / \sum w(F_0^2)^2]^{1/2}.$$

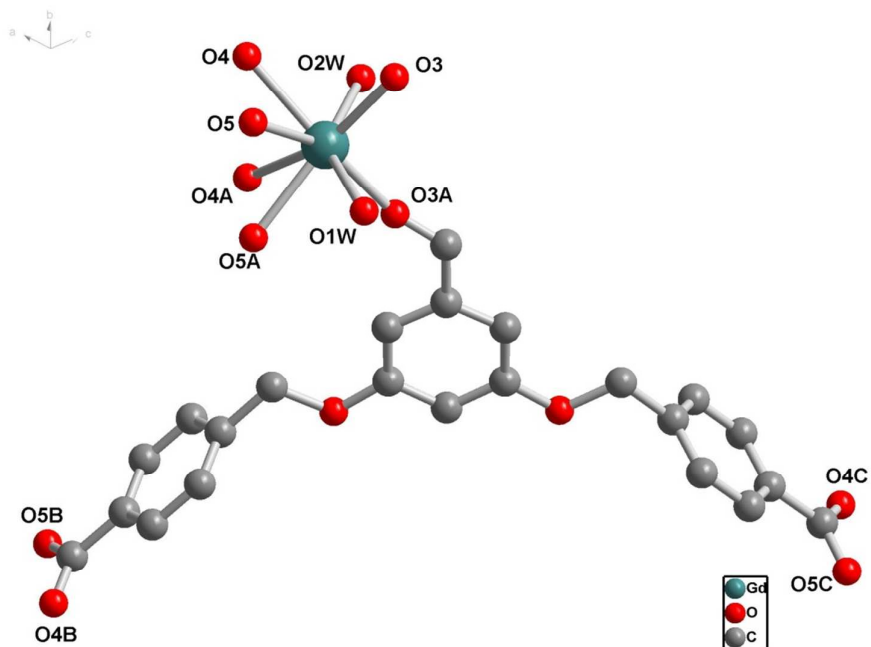


Figure S3. Representation of the La(III) coordination environments of compound $\text{Gd}(\text{CPOMBA})(\text{H}_2\text{O})_2 \cdot n\text{H}_2\text{O}$. Symmetry operation: A) $x, 1-y, z$; B) $0.5-x, -0.5+y, 1-z$; C) $-0.5+x, -0.5+y, 1+z$. All carbon H atoms and lattice solvent molecules are omitted for clarity

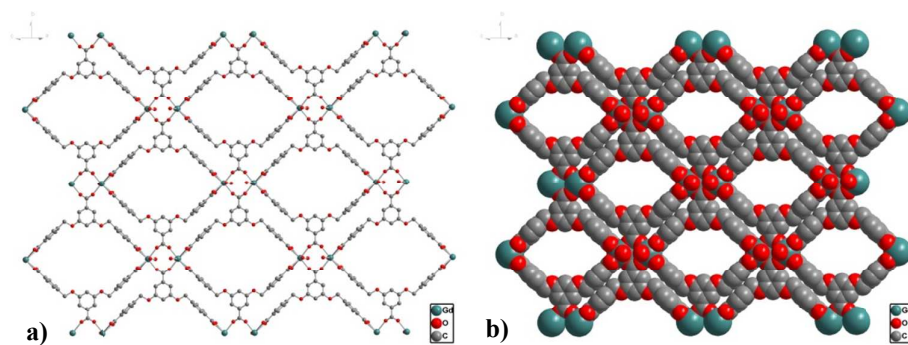


Figure S4. a) 2D layer structure of $\text{Gd}(\text{CPOMBA})(\text{H}_2\text{O})_2 \cdot n\text{H}_2\text{O}$. H atoms were omitted for clarity. b) Space-filling representation of the 2D structure.

Section S4. PXRD patterns and IR spectra of partial MOF

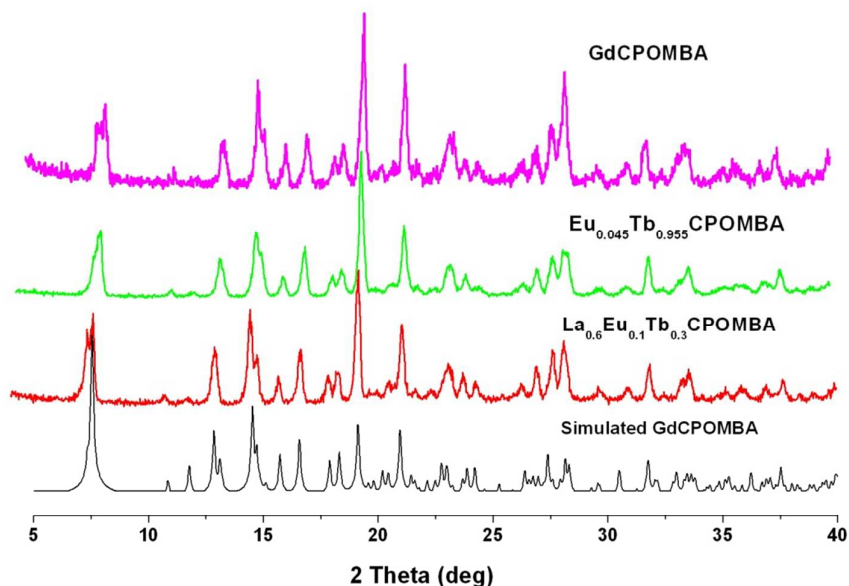


Figure S5. Powder X-ray diffraction patterns of simulated Gd(CPOMBA)(H₂O)₂·nH₂O and as-synthesized Gd(CPOMBA)(H₂O)₂·nH₂O, Eu_{0.045}Tb_{0.955}CPOMBA and La_{0.6}Eu_{0.1}Tb_{0.3}CPOMBA.

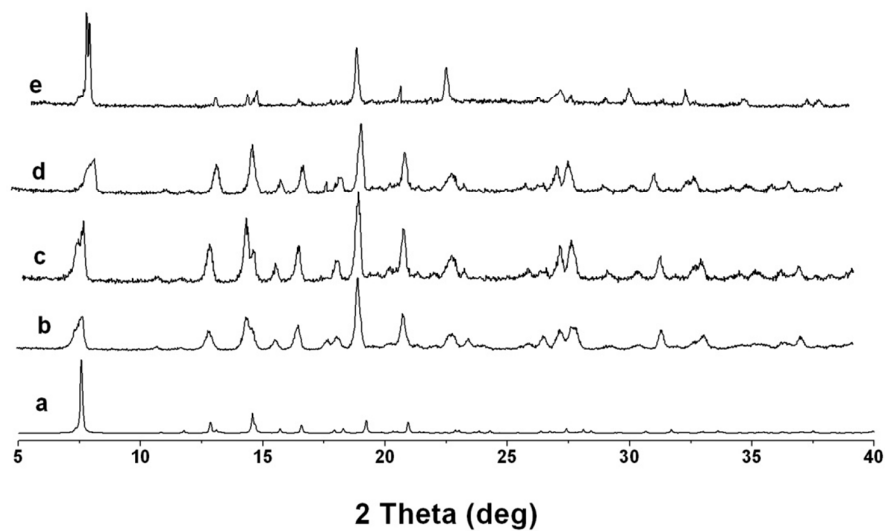


Figure S6. X-ray powder patterns of Eu_{0.045}Tb_{0.955}CPOMBA: a) calculation from the single-crystal structure of Eu(CPOMBA)(H₂O)₂·nH₂O; b) an as-made

sample of $\text{Eu}_{0.045}\text{Tb}_{0.955}\text{CPOMBA}$ at Rt; c) sample from (b) after treatment at 100 °C for 24 h; d) sample from (b) after treatment in boiling water for 24 h; e) sample from (b) after treatment at 150 °C for 48 h.

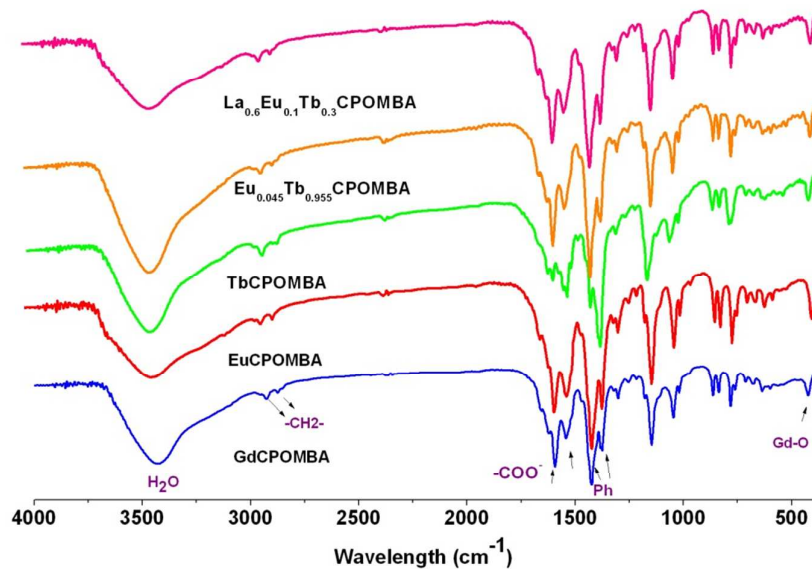
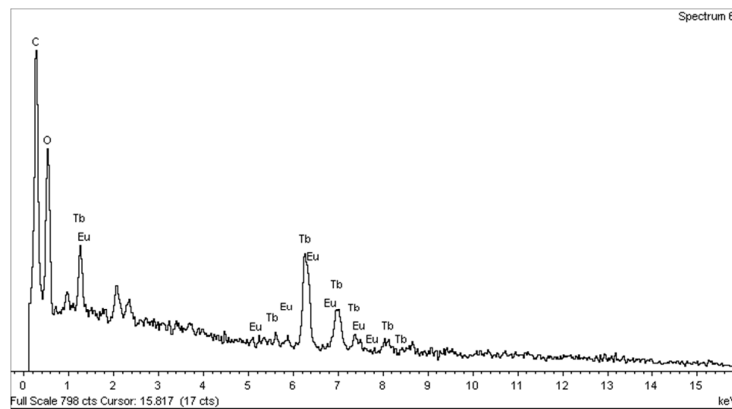
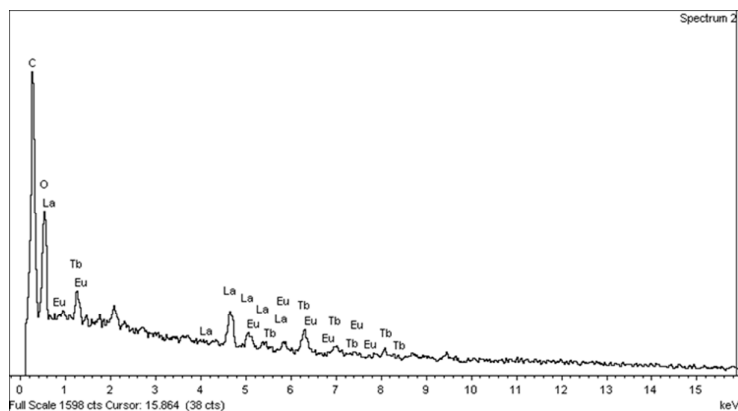


Figure S7. IR spectra of various $\text{Ln}(\text{CPOMBA})(\text{H}_2\text{O})_2$ MOFs.

Section S5. EDS spectrum of the doping LnMOF



(a)



(b)

Figure S8. (a) EDS spectrum of $\text{Eu}_{0.045}\text{Tb}_{0.955}\text{CPOMBA}$ and (b) $\text{La}_{0.6}\text{Eu}_{0.1}\text{Tb}_{0.3}\text{CPOMBA}$ (bottom) acquired in SEM.

Section S6. Thermal gravimetric analysis of $\text{Gd}(\text{CPOMBA})(\text{H}_2\text{O})_2 \cdot n\text{H}_2\text{O}$

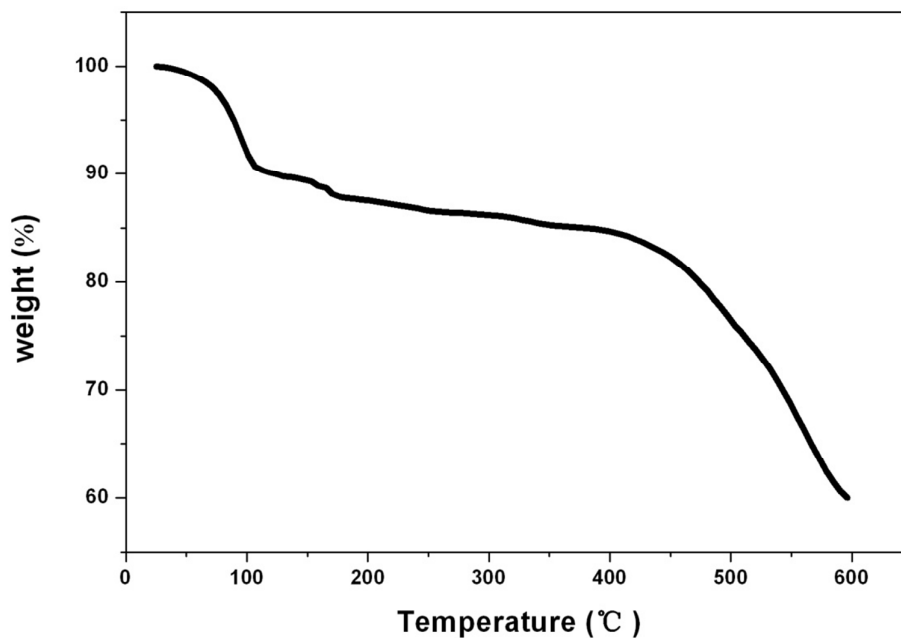


Figure S9. Representative TGA curve of compound $\text{Gd}(\text{CPOMBA})(\text{H}_2\text{O})_2 \cdot n\text{H}_2\text{O}$.

Section S7. Excitation and Emission spectra of free ligand single and doping LnMOF

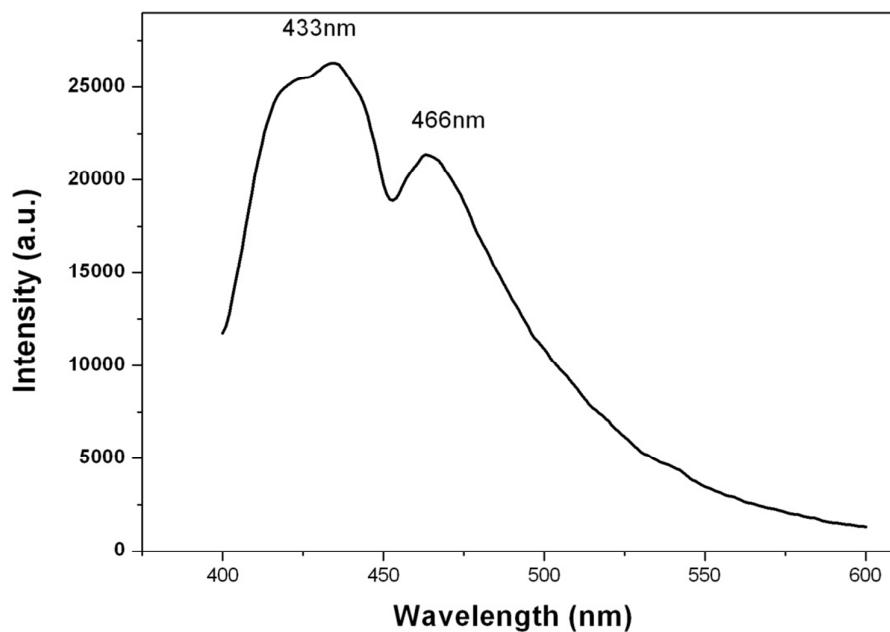


Figure S10. Emission spectra of La(CPOMBA)(H₂O)₂·nH₂O under excitation of 362nm

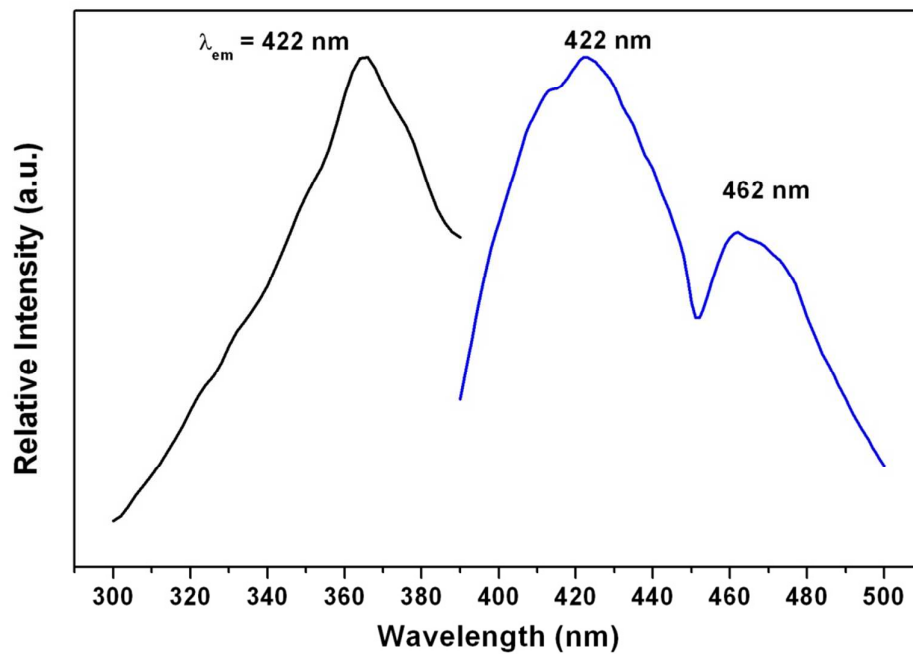


Figure S11. Excitation and emission spectra of free ligand H₃CPOMBA

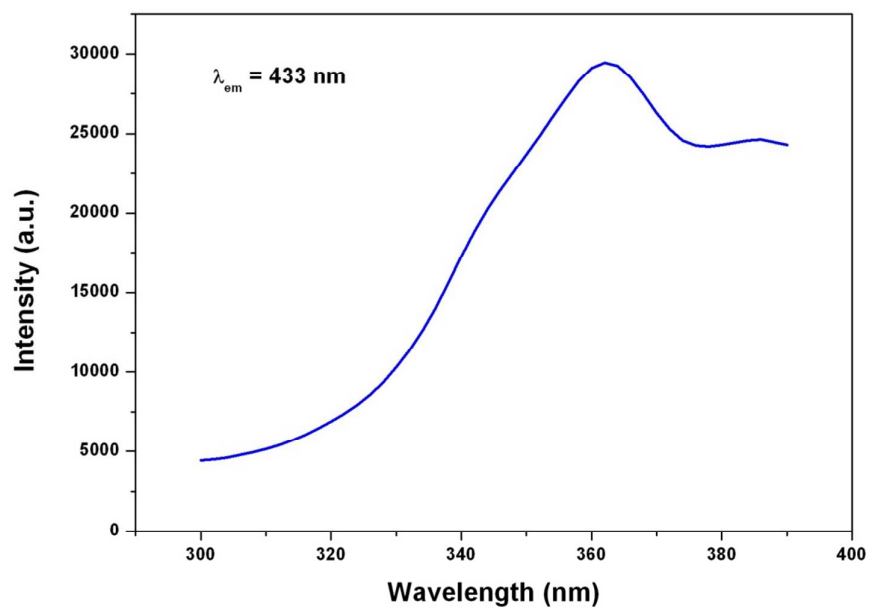


Figure S12. Excitation spectra of LaCPOMBA

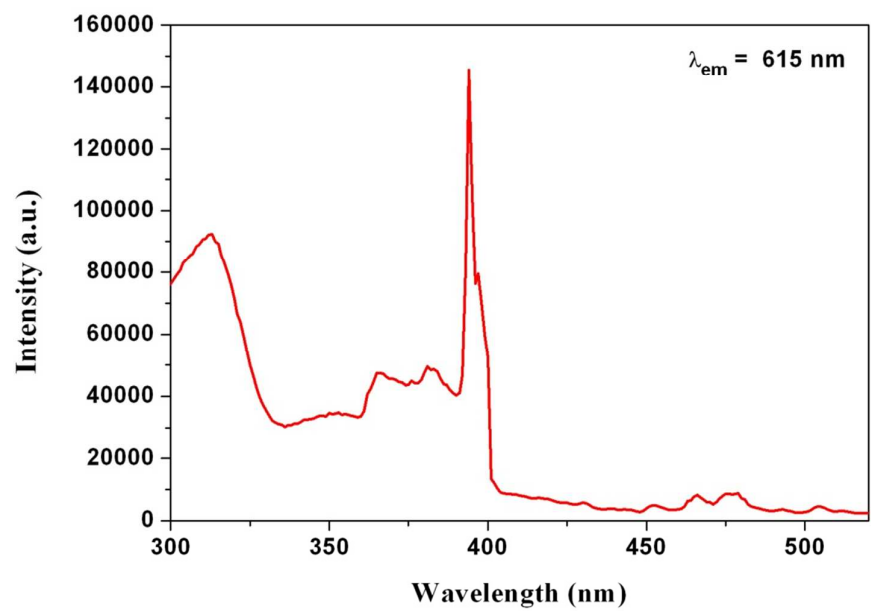


Figure S13. Excitation spectra of EuCPOMBA

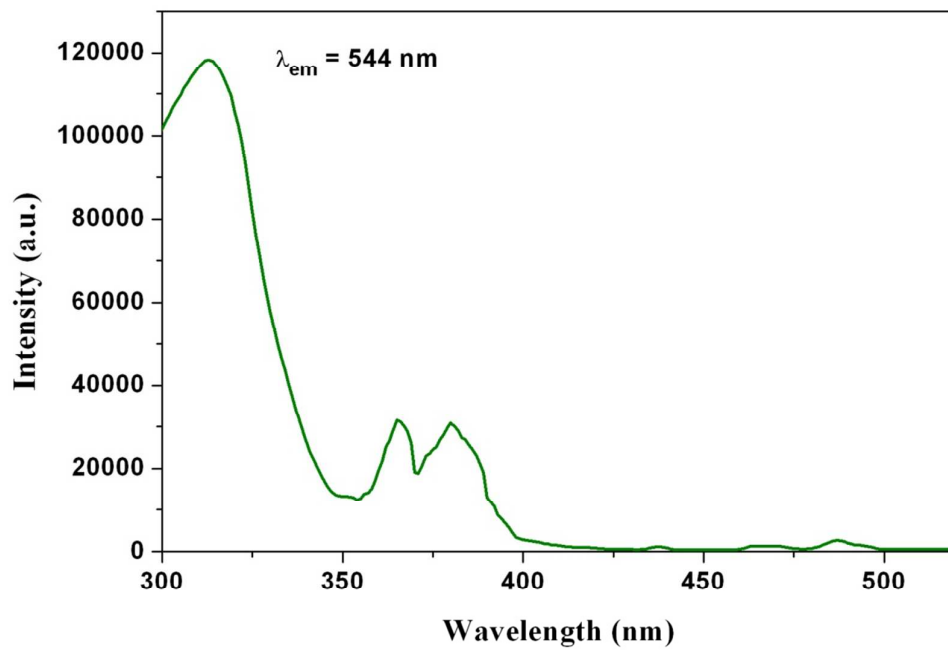


Figure S14. Excitation spectra of TbCPOMBA

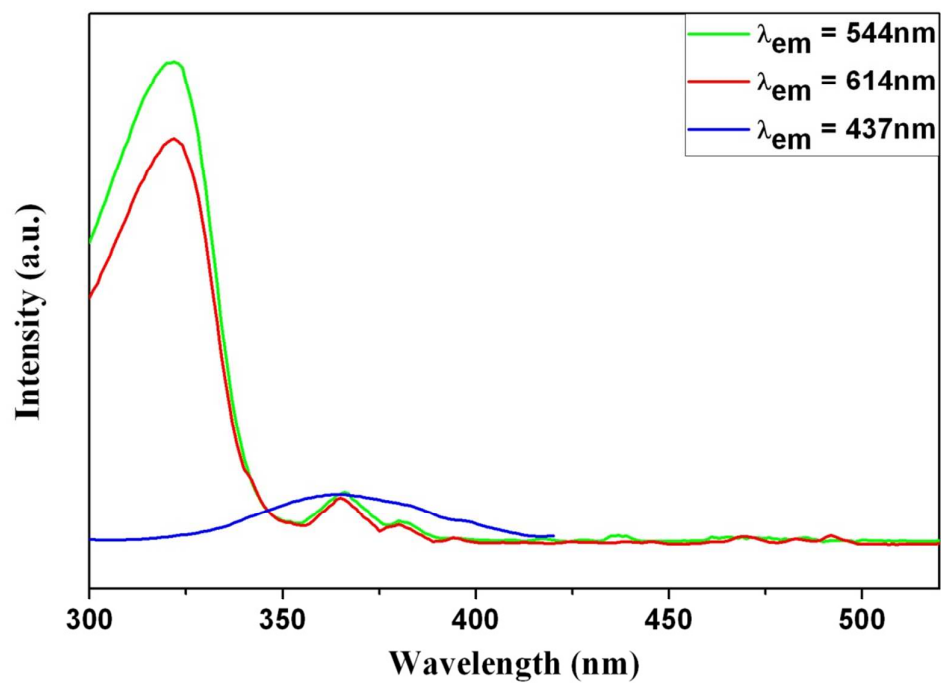


Figure S15. Excitation spectra of Eu_{0.045}Tb_{0.955}CPOMBA

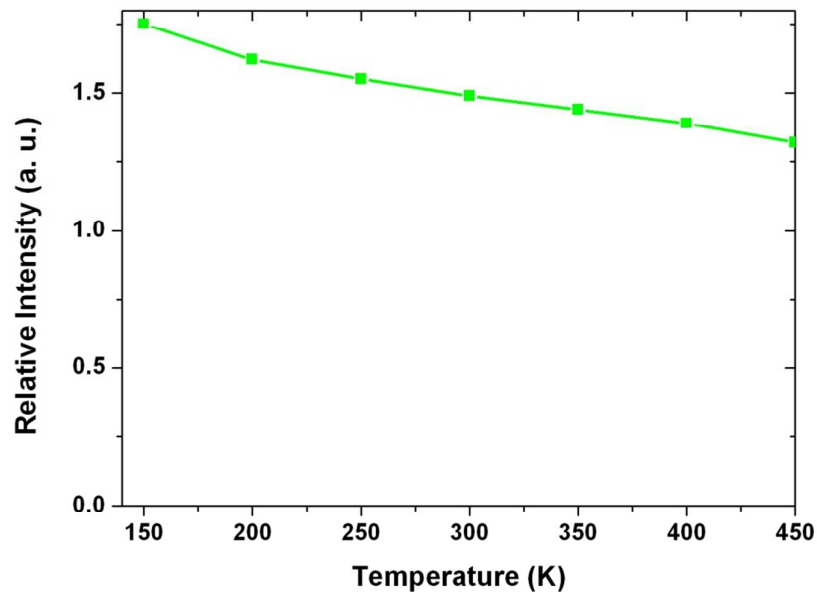


Figure S16. Emission spectra ($\lambda_{\text{ex}} = 365\text{nm}$) of $\text{Eu}_{0.045}\text{Tb}_{0.955}\text{CPOMBA}$ at different temperature.

Section S8. CIE coordinates of doping LnMOF

Table S4. CIE coordinates for the $\text{Eu}_x\text{Tb}_{1-x}\text{-CPOMBA}$ ($x = 0\text{-}20$ mol%) excited at 324 nm.

Molar ratio of $\text{Eu}^{3+}:\text{Tb}^{3+}$	CIE coordinates
0.5% : 99.5%	(0.2989, 0.5882)
4.5% : 95.5%	(0.4264, 0.4913)
7.5% : 99%	(0.488, 0.4441)
10% : 90%	(0.5093, 0.4342)
15% : 85%	(0.5735, 0.4003)
20% : 80%	(0.5771, 0.3861)

Table S5. CIE coordinates for the $\text{Eu}_{0.045}\text{Tb}_{0.955}\text{CPOMBA}$ excited from 330 nm to 370nm.

Wavelength of excitation	CIE coordinates
330nm	(0.4661, 0.4775)
340nm	(0.4589, 0.4521)
350nm	(0.419, 0.3983)
355nm	(0.3774, 0.3526)
360nm	(0.3636, 0.3469)
365nm	(0.333, 0.32)
370nm	(0.2771, 0.2598)

Table S6. CIE coordinates for the $\text{La}_x\text{Eu}_y\text{Tb}_{1-x-y}\text{-CPOMBA}$ excited at 324 nm.

Molar ratio of $\text{La}^{3+}:\text{Eu}^{3+}:\text{Tb}^{3+}$	CIE coordinates
94%: 3%: 3%	(0.3476, 0.5216)
60%: 10%: 30%	(0.3919, 0.5240)
60%: 22%: 18%	(0.4354, 0.4633)
60%: 25%: 15%	(0.4971, 0.421)
55%: 25%: 15%	(0.4657, 0.4554)
35%: 30%: 25%	(0.55, 0.4052)
25%: 40%: 35%	(0.5957, 0.3747)

Table S7. CIE coordinates for the $\text{La}_{0.6}\text{Eu}_{0.1}\text{Tb}_{0.3}$ -CPOMBA excited from 330 nm to 390nm.

Wavelength of excitation	CIE coordinates
330nm	(0.397, 0.5228)
340nm	(0.3928, 0.4862)
350nm	(0.3783, 0.4027)
360nm	(0.3569, 0.3567)
370nm	(0.3377, 0.3481)
380nm	(0.323, 0.326)
390nm	(0.3194, 0.3098)

Section S9. Photoluminescent decay curve of doping LnMOF

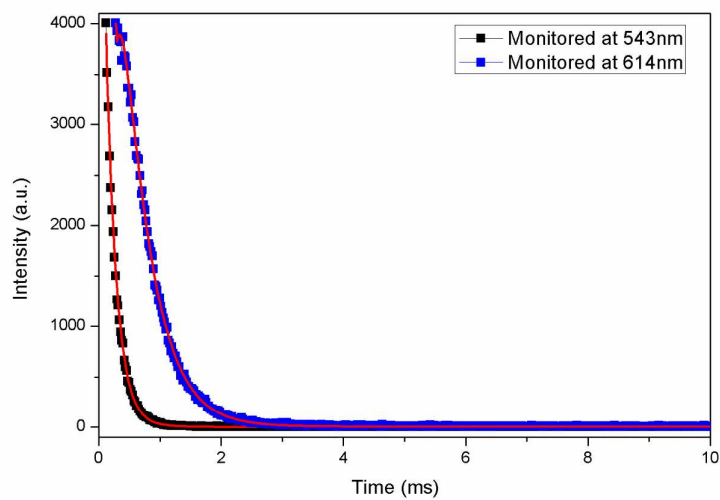


Figure S17. The PL decay curve of $\text{Eu}_{0.045}\text{Tb}_{0.955}$ CPOMBA recorded at room

temperature with emission monitored by the $^5D_4 \rightarrow ^7F_5$ transition at 543 nm and the $^5D_0 \rightarrow ^7F_2$ transition at 614 nm ($\lambda_{\text{ex}} = 365$ nm). The red lines are the best fit to the data using a two-exponential function, giving the average values of $\tau_{\text{Tb}^{3+}} = 0.176$ ms and $\tau_{\text{Eu}^{3+}} = 0.656$ ms.

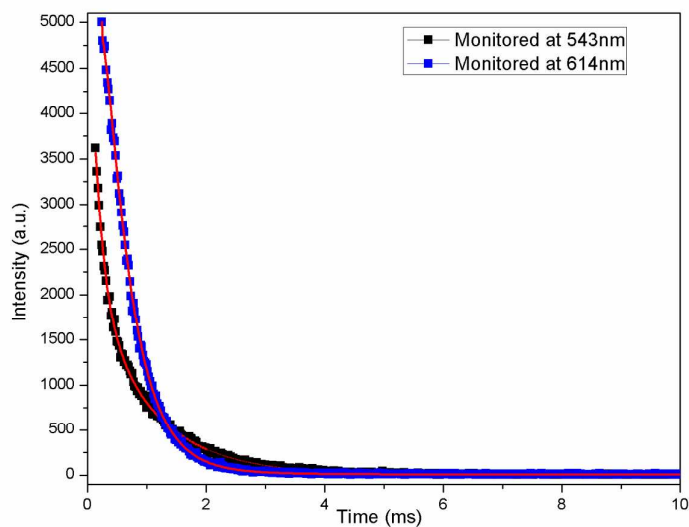


Figure S18 The PL decay curve of $\text{La}_{0.6}\text{Eu}_{0.1}\text{Tb}_{0.3}\text{-CPOMBA}$ recorded at room temperature with emission monitored by the $^5D_4 \rightarrow ^7F_5$ transition at 543 nm and the $^5D_0 \rightarrow ^7F_2$ transition at 614 nm ($\lambda_{\text{ex}} = 380$ nm). The red lines are the best fit to the data using a two-exponential function, giving the average values of $\tau_{\text{Tb}^{3+}} = 0.579$ ms and $\tau_{\text{Eu}^{3+}} = 0.556$ ms.

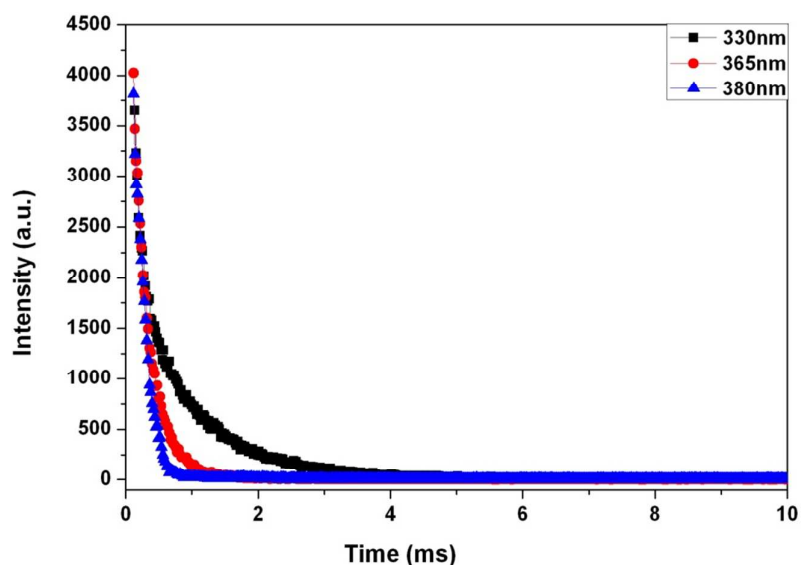


Figure S19. The PL decay curve of $\text{Eu}_{0.045}\text{Tb}_{0.955}\text{CPOMBA}$ recorded at room temperature with emission monitored by the ${}^5\text{D}_4 \rightarrow {}^7\text{F}_5$ transition at 543 nm under different excitation wavelength (330nm, 365nm, 380nm).

Section S10 quantum yield of doping LnMOF

The measurement and calculation for quantum yield for $\text{Eu}_{0.045}\text{Tb}_{0.955}\text{CPOMBA}/\text{La}_{0.6}\text{Eu}_{0.1}\text{Tb}_{0.3}\text{CPOMBA}$ sample

- Measure the blank laser excitation line (E_{blank}) from 360 to 370 nm for $\text{Eu}_{0.045}\text{Tb}_{0.955}\text{CPOMBA}$ and from 375 to 385nm for $\text{La}_{0.6}\text{Eu}_{0.1}\text{Tb}_{0.3}\text{CPOMBA}$.
- Put the sample on the sample hold in the integrating sphere. Then the emission spectra in the range of 400-705 nm were collected. Every spectrum was scanned at least 5 times. The spectrum from 360 to 370 nm (or from 375nm to 385nm) is E_S , and from 400 to 705 nm is L_S , respectively.
- Then the quantum yields (QY) are calculated with the software supplied by the manufacturer based on the equation 1. The η here refers to the QY of the emission from 400 to 705 nm.

$$\eta = \frac{\int L_S}{\int E_{\text{blank}} - \int E_S}$$

The raw data used for the calculation of quantum yield of $\text{Eu}_{0.045}\text{Tb}_{0.955}\text{CPOMBA}/\text{La}_{0.6}\text{Eu}_{0.1}\text{Tb}_{0.3}\text{CPOMBA}$ sample are listed in the following table S8.

Table S8. The raw data for the calculation of $\text{Eu}_{0.045}\text{Tb}_{0.955}\text{CPOMBA}/\text{La}_{0.6}\text{Eu}_{0.1}\text{Tb}_{0.3}\text{CPOMBA}$ sample

sample	$\int E_{\text{blank}}$	$\int E_S$	$\int L_S$	η (%)
$\text{Eu}_{0.045}\text{Tb}_{0.955}\text{CPOMBA}$	451911.5	300790.4	22668.1	15±0.2
$\text{La}_{0.6}\text{Eu}_{0.1}\text{Tb}_{0.3}\text{CPOMBA}$	417582.8	284368.5	19182.8	14.4±0.3

Section S11. Photographs of LEDs and optical photographs of crystal

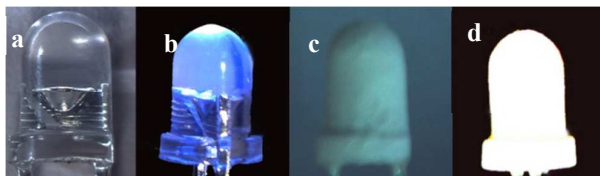


Figure S20. Photographs of LEDs: A 3 mm reference UV LED (365nm) turned off (a) and on (b); the same LED coated with a thin layer of compound $\text{Eu}_{0.045}\text{Tb}_{0.955}\text{CPOMBA}$ turned off (c) and on (d).

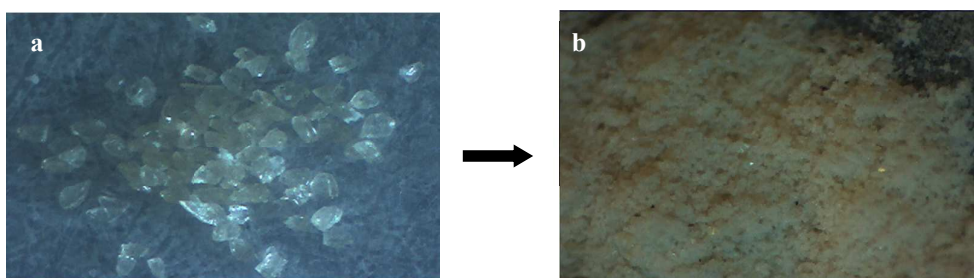


Figure S21. Optical photographs of representative $\text{Eu}_{0.045}\text{Tb}_{0.955}\text{CPOMBA}$ crystal sample in natural light before (a) and after (b) grinding.

Section S12. Fabrication of UV WLED

Method I. As described by He et al², crystal compound $\text{Eu}_{0.045}\text{Tb}_{0.955}\text{CPOMBA}$ (5mg) was put into an agate mortar and manually ground with the pestle until the crystal particle completely become powder. Following on this, 1mL anhydrous ethanol was added into the mortar, which was continued to be ground. When the solid-liquid mixture was uniformly blended, a commercially available n-UV LED lamp (365nm) was covered with the mixture by a dropper. After several times repeating on the above procure, an even coatings on the WLED was fabricated, which was used directly after drying.

Method II. white LEDs with various concentrations and particle size (Table 1) were fabricated with 365nm GaN chip and $\text{Eu}_{0.045}\text{Tb}_{0.955}\text{CPOMBA}$ phosphor. The chip was first fixed at the center of LED substrate. The 365nm UV chip was coated on different proportion mixture of phosphor and silicone, and baked 30 minutes in 160°C oven, then filled lens up with silicone (different from aforementioned silicone) and baked 2 h in 120°C oven. The photoelectric properties of the fabricated LEDs were measured by an integrating sphere spectroradiometer system (HP-8000, Hopoo, China).

References

- (1) Runge, E.; Gross, E. K. U. Density-Functional Theory for Time-Dependent Systems, *Phys. Rev. Lett.* **1984**, *52*, 997-1000.
- (2) He, J.; Zeller, M.; Hunter, A. D.; Xu, Z. White Light Emission and Second Harmonic Generation from Secondary Group Participation (SGP) in a Coordination Network. *J. Am. Chem. Soc.* **2012**, *134*, 1553-1559.